INTERNATIONAL JOURNAL OF PRECISION ENGINEERING AND MANUFACTURING-GREEN TECHNOLOGY Vol. 2, No. 4, pp. 325-331 OCTOBER 2015 / 325
DOI: 10.1007/s40684-015-0039-2 ISSN 2288-6206 (Print) / ISSN 2198-0810 (Online)

# Dry Rotary Swaging – Approaches for Lubricant Free Process Design

**Florian Böhmermann[1,#], Henning Hasselbruch[2], Marius Herrmann[3], Oltmann Riemer[1], Andreas Mehner[2], Hans-Werner Zoch[2], and Bernd Kuhfuss[3]**

1 LFM Laboratory for Precision Machining, University of Bremen, Badgasteiner Straße 2, 28359 Bremen, Germany
2 IWT Foundation Institute for Material Science, Badgasteiner Straße 3, 28359 Bremen, Germany
3 bime Bremen Institute for Mechanical Engineering, University of Bremen, Badgasteiner Straße 1, 28359 Bremen, Germany
# Corresponding Author / E-mail: boehmermann@lfm.uni-bremen.de, TEL: +49-421-218-51124, FAX: +49-421-218-51119

KEYWORDS: Bulk metal forming, Dry metal forming, Radial forging

*Rotary swaging is an incremental cold forming process and allows for the cost effective manufacture of cylindrical light weight components such as rods or hollow shafts. The process has a widespread use particularly in the automotive industry for example for the manufacture of axles and steering spindles. Besides the generation of desired geometries, rotary swaging offers the advantage of improved work piece material properties due to strain hardening and furthermore the generation of variable wall thicknesses for hollow shafts, and therefore an optimal use of material resources. Nowadays rotary swaging is carried out under the use of extensive amounts of lubricant. Main functions of the lubricant are the cooling of work piece and tools, washing out of wear particles from the forming zone and process lubrication in general. Before further processing, remaining lubricant mandatorily needs to be cleaned off the work piece, increasing the costs per unit significantly. Thus, an enhancement of rotary swaging towards a lubricant free process, i.e. a dry rotary swaging, is seen to be highly innovative, both under economic and ecological aspects. However, a lubricant free process design exhibits considerably modified frictional conditions, compared to a conventional process layout. This leads to changes in the power.*

Manuscript received: February 24, 2015 / Revised: June 12, 2015 / Accepted: July 19, 2015

**NOMENCLATURE**

$d_0$ : initial diameter of work piece
$d_1$ : final diameter of work piece
$E_{IT}$ : elastic indentation modulus
$F_A$ : axial reaction force
$F_{A,max}$ : maximum reaction force
$F_f$ : feed force
$F_R$ : radial forming force
$F_{RI}$ : radial force in the reduction zone
$F_{RII}$ : radial force in the calibration zone
$F_{R,max}$ : maximum excitation force
$H_{IT}$ : hardness
$h_t$ : stroke height
$r_0$ : initial radius of work piece
$r_1$ : final radius of work piece
Sa : arithmetical mean height
$v_f$ : feed velocity
$\alpha$ : tool angle
$\mu_{Red}$ : friction coefficient in the reduction zone
$\mu_{Cal}$ : friction coefficient in the calibration zone

## 1. Introduction

Rotary swaging allows for the reduction of the diameter of a work piece by incremental forming. The principle setup of the infeed rotary swaging process is shown in Fig. 1. The work piece is axially fed into the swaging unit with the feed force $F_f$ and then machined due to the oscillating movement of the tools. The radial forming force $F_{RI}$ in the reduction zone is resulting in an axial reaction force $F_A$ counteracting the feed force. The magnitude of the axial reaction force directly depends on the tool geometry and the frictional conditions in among

the tools and the work piece. Generally rotary swaging is associated with considerably high process forces and contact pressures per unit area, resulting in high frictional shear stresses.[1]

Furthermore, the forming work applied to the work piece results in an increased work piece surface area. The newly formed surfaces are considered to be free of protective oxide layers.[2] Both, high shear stresses and oxide layer free surfaces provoke abrasive and adhesive wear of the tools and a reduction of surface quality or even a damage of the work piece material. In conventional rotary swaging, the lubricant is a key component for process reliability and desired work piece quality by providing a hydrodynamic separation of the tools and the work piece.[3] The extend use of lubricant, however, leads to a considerably reduced friction between tools and work piece within the reduction zone resulting in a high axial reaction force making the process unworkable. Commercially available rotary swaging tools, therefore, exhibit a thermal sprayed layer of tungsten carbide with a rough surface finish. This increases the effective friction between the tools and the work piece leading to a reduction of the axial reaction force. An enhancement of rotary swaging towards a lubricant free process, i.e. a dry rotary swaging, is seen to be highly innovative, both under economic and ecological aspects. However, a lubricant free process design exhibits considerably modified frictional conditions, compared to a conventional process layout. This can be encountered by adapted tool surfaces, substituting the functions of the lubricant. Newly developed hard coatings, e.g. can provide both reduced friction and protection of tools against abrasive and adhesive wear when applied to the tools surfaces. Structured tool surfaces can be applied for friction control in the reduction zone. However, the testing and optimization of such adapted tools is complex and time consuming when carried out within the actual rotary swaging process. Here, the modelling of rotary swaging is assumed to strongly support the development of dry rotary swaging by cutting down the number of experiments through process simulation under various conditions. This work presents an interdisciplinary scientific approach contributing to a successful design of lubricant free rotary swaging by the functionalization of tool surfaces. The approach comprises at first: the development of tungsten doped a-C:H hard coatings for the reduction of abrasive and adhesive wear of the tools; second: the structuring of the rotary swaging tool surfaces for friction and process forces control; and third: for general understanding and design of dry rotary swaging process a FE modelling and simulation to be used for the pre-calculation of process forces and energy demand (see Fig. 2). Each of the methodologies and first results of investigations are highlighted in the subsequent sections.

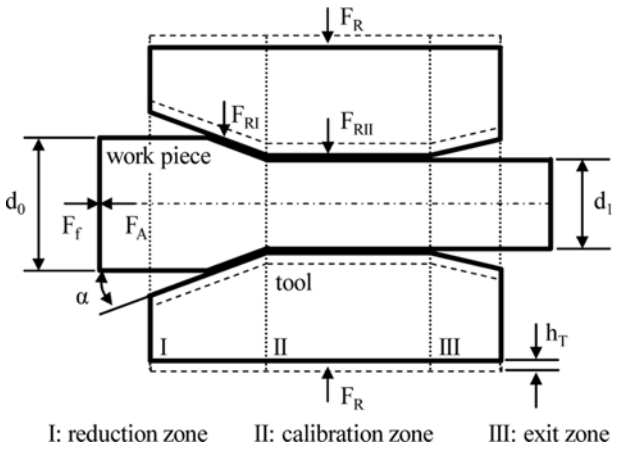


Fig. 1 Cross-Sectional view of the infeed rotary swaging process setup and process forces

## 2. Experiments

All investigations refer to an exemplary rotary swaging process that is carried out on a Felss HE-32 V machine tool. The swaging frequency is depending on the rotational speed of the swaging unit. The stroke height $h_t$ of the tools is 1 mm. The applied tool design for the experiments exhibits a tool angle of $\alpha = 10°$ and allows for the diameter reduction of rod and hollow shafts from $d_0 = 20$ mm down to $d_1 = 15$ mm. Two different work piece materials are applied: steel S235 and AlMgSi0.5 aluminum alloy. The work pieces are fed into the swaging unit at the feed velocity $v_f$ by a linear direct driven feed unit with a maximum feed force $F_f$ of 20 000 N. An integrated force transducer in the feed unit allows for the measurement of the axial reaction force $F_A$.

## 3. Approaches for a Lubricant Free Process Design

### 3.1 Hard Coated Rotary Swaging Tools

The tool wear in cold forming processes can effectively be reduced with the deposition of hard coatings such as CrN, TiN, TiAlN, TiCn or low friction DLC coatings (diamond like carbon). A dominant role plays the surface roughness and the friction between the work piece and tool surfaces for lubricant free process conditions. In particular, the best overall performance and promising wear characteristics are

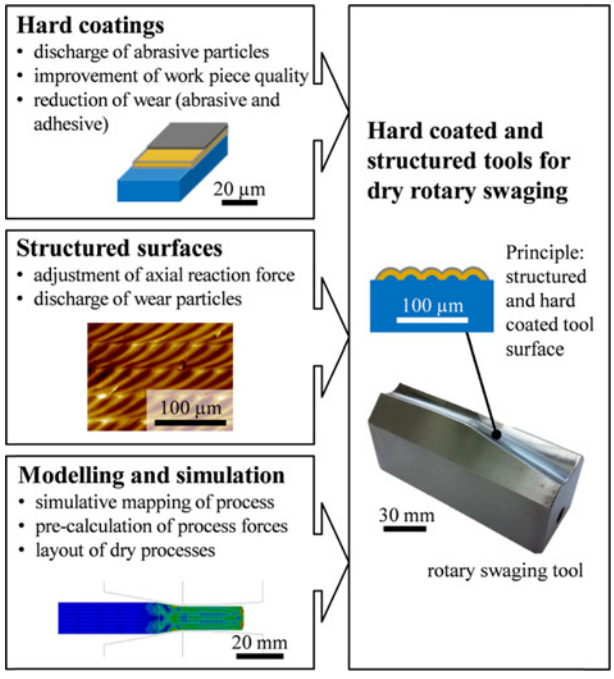


Fig. 2 Interdisciplinary approach for providing a lubricant free rotary swaging process

provided by coatings with low friction coefficients, e.g. the DLC coatings.[4] The low friction of DLC coatings is caused by the formation of graphitization layers in nanometer scale. This formation of the so-called tribolayer depends on the sliding velocity and pressure per unit area.[5] The tendency to adhesion is a further important aspect which depends on chemical adhesion reactions between the DLC coating and the work piece material. Due to the roughness of the coating in the forming zone, adhesion can also caused by micro toothing effects. Compared to the above mentioned nitride hard coatings, DLC coatings show a lower tendency to adhesion against aluminum and steel materials.[6] This lower tendency to cold welding can be explained by the saturation of carbon bonds by OH groups or hydrogen on the surfaces.[2] Besides the tribological properties, the mechanical properties of coatings are of great importance. Dynamic loads with high pressure per unit area and shear stress are applied to the tool's surfaces during rotary swaging. For this reason, the hard coatings require sufficient fracture toughness. Both, high hardness and increased fracture toughness are needed to reduce abrasive wear and wear due to fatigue. Amorphous carbon coatings like diamonds (a-C:H) are mainly characterized by low tendency to adhesion and low friction in contact with aluminum and steel as well as high hardness.[7,8] However, a-C:H coatings generally have low bearing strength and low overload protection.[2] Local overloads may result in premature a-C:H coating failure, e.g. delamination, due to the induced high impact stresses.[9] Hard adhesion Cr/CrN-interlayers as shown in Fig. 3 are used to overcome this so-called "eggshell effect."

As shown in Fig. 3(c), an additional a-C:H interlayer doped with tungsten (a-C:H:W) is used to improve the fracture toughness and the resistance against wear due to fatigue. For this purpose, a graded tungsten carbide interlayer will act as a mediator between the Cr/CrN adhesion-layer and the hard and low friction a-C:H-layer on top. It is expected, that doping with tungsten improves the adhesion and increases the toughness.[10,11] Therefore, a Cr/CrN/a-C:H layer system, acting as a reference layer, is stepwise modified to a tungsten doped multilayer system with an a-C:H top layer as shown in Fig. 3.

Steel discs with a diameter of 32 mm and a thickness of 4 mm were made of cold working steel 1.2379 for the coating experiments. For this purpose, the overall hardness was set to 62 ± 2 HRC, corresponding to the target hardness for common rotary swaging tools. After heat treatment the specimen were first ground, lapped and then polished to an average area roughness Sa of about 4 nm which was measured with an atomic force microscope, type Veeco Explorer. The discs were cleaned in an Amsonic ECS 40 cleaning machine with a precision cleaning medium Zestron®VD before deposition. The cleaning steps contain ultrasonic, spray and steam cleaning and are finished by drying in a vacuum. A CemeCon CC800/9 SinOx magnetron sputtering device with a total of four cathodes was used for carrying out the deposition experiments. One cathode was implemented with a chromium target which operated in direct current (DC) mode for the deposition of the Cr/CrN adhesion layer according to the reference layer system as shown in Fig. 3(a). Furthermore, two cathodes operated in a bipolar pulsed-DS power mode which were implemented with graphite targets for the deposition of the a-C:H:W and a-C:H layers. According to the tungsten doped layer systems shown in Figs. 3(b) and 3(c) the fourth cathode was implemented with a tungsten-carbide target, also operated in DC mode. Three different processes were carried out in total: Cr/CrN/CrCx/a-C:H reference layer system without tungsten, Cr/CrN/WCx+CrCx/a-C:H:W and Cr/CrN/WCx+CrCx/a-C:H:W/ a-C:H layer system with a low friction a-C:H-top layer.

Both, the chromium cathode and the two graphite cathodes operated in power mode with a power of 2 kW and the WC cathode with a power of 1 kW. The entire deposition process is separated in three phases: the heating phase, the plasma etching and the various deposition phases depending on deposition parameters. The duration of the heating phase is 1000 s, heated with an average power of 15 kW and started at a base pressure between 1 mPa and 5 mPa. The duration of plasma etching was set to 500 s, with an argon flow rate of 300 sccm respectively 75 sccm of krypton and a pulsed bias voltage of -650 V. A constant nitrogen flow rate of 15 sccm was used for the deposition of the CrN interlayer. Six Rockwell C indentations were performed on each sample to evaluate the adhesion of these for attempts according to VDI 3198 (see Fig. 4).

A Fischerscope H100C micro hardness measuring system was used for the determination of the indentation hardness and elastic indentation modulus. 25 measurements on each specimen were performed for a statistical coverage, with the indentation force set to 10 mN and the indentation time to 10 s. For measuring the coating thickness a mean value of five ball grinding experiments was carried out. The roughness Sa was measured on a 100 $\mu$m × 100 $\mu$m area using an Veeco Instruments Explorer atomic force microscope. The results of the

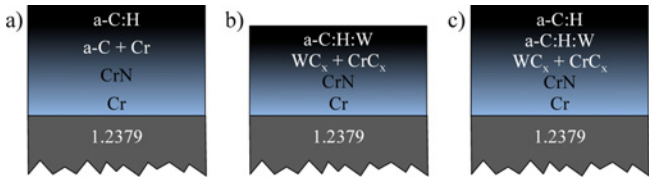


Fig. 3 Multilayer systems; (a) Reference layer Cr/CrN/C+Cr/a-C:H (b) Cr/CrN/WCx + CrCx/a-C:H:W (c) Cr/CrN/WCx + CrCx/a-C:H:W/a-C:H

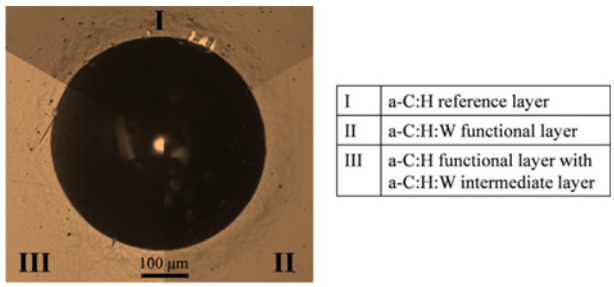


Fig. 4 Composite photoghraphy of three individual Rockwell-Cindentations on different hard coated multilayer systems

Table 1 Experimental results of the different coating variants compared with uncoated 1.2379 steel

| | un-coated | I | II | III |
|---|---|---|---|---|
| $H_{IT0,01/10/10}$ [GPa] | 11.8 | 21.3 | 18.0 | 18.2 |
| $E_{IT0,01/10/10}$ [GPa] | 272 | 190 | 201 | 177 |
| HF1-6 | - | 2.0 | 1.3 | 1.6 |
| Roughness Sa [nm] | 3.7 | 5.3 | 5.1 | 5.3 |
| Thickness [$\mu$m] | - | 1.77 | 2.46 | 1.75 |

experiments are shown in Table 1.

The first experimental results confirm the above mentioned hypotheses, that doping with tungsten can contribute to an improvement of adhesion. The variants II and III are subjects of current research.

### 3.2 Structured Tool Surfaces

Micro structured surfaces of forming tools can influence the tribological function and therefore can be applied to control the forming process itself e.g. through affecting the material flow. The functionality of these structures can be set into relation with their geometrical dimensions: macroscopic structures (feature size of about 100 µm and above) can influence the direction of the load transmission to the work piece. A theoretical approach of structured rotary swaging tools in order to reduce the axial reaction force $F_A$ was shown before.[12] In the case of sheet metal forming the tribological effectiveness of surface structures was demonstrated. Drawing tools exhibiting grooves perpendicular to the drawing direction of the sheet material lead to an elastic deformation of the work piece material and allow for an increase of friction.[13] Such grooves can be characterized as mesoscopic structures with a feature size of about 30 micrometers to about 200 micrometer. Microscopic structures, e.g. pockets with a depth of several micrometers, usually serve as lubrication reservoirs in conventional forming processes to achieve a hydrodynamic separation of the tool and the work piece and with this reduce friction and wear.[14] In the case of dry forming other effects need to be taken into consideration, which predetermine the frictional properties. Generally, friction is based on energy dissipation due to four different physical mechanisms: adhesion, elastic hysteresis, plastic deformation of roughness asperities, and abrasion due to plowing of wear particles generated within the process. Generally, the presence of micro structures on surfaces can reduce the friction due to a reduced area of contact in tribological contact.[15] Furthermore, micro structures could reduce the friction under dry conditions by containing wear particles that otherwise provoke plowing and therefore higher friction.[16]

Structured tool surfaces will contribute to the development of a lubricant free rotary swaging process. A successful application of structures on rotary swaging tools implicates the understanding of the predominant friction regime and the effectiveness of the friction in dependence on areal roughness parameters (ISO 25178 standard). However, the tribological investigation of tools with structured surfaces within real rotary swaging processes is strongly limited due to the accessibility to e.g. force measurement equipment and in practice requires the manufacture of a new set of rotary swaging tools for each approach.

For the tribological investigation of micro structured samples under conditions similar to the real swaging process a new test rig has been developed mimicking typical contact geometries of the tools and work piece as well as impact loads resulting in high contact pressure per unit area. The contact pressures per unit area to be applied have been derived from the simulation results explained in detail in Section 3.3. The setup for tribological investigations is shown in Fig. 5. A variable impacting mass is used to apply an impact load to the work piece sample holder containing samples made of the work piece material. The counteracting structured tool sample made from hardened tool steel is attached to the tool sample holder. The samples have an effective tribological contact area of 100 $mm^2$ and are interacting under a tool angle of $\alpha = 10^o$ according to the typical tool angles $\alpha$ at the reduction zone of rotary swaging tools. By varying the impacting mass contact pressures of 1000 to 7200 $N/mm^2$ can be realized. Fig. 6 shows a detailed view of both sample holders and inserted samples of micro structured tool and work piece material. The impact of the falling mass (vertical, i.e. the force $F_R$ in radial direction in rotary swaging) causes a reaction force (horizontal, i.e. the force $F_A$ in axial direction in rotary swaging) acting against the deflection measurement unit. The deflection measurement unit comprises a spring assembly and a dial indicator with trailing hand, allowing for an indirect measurement of the maximum axial reaction force $F_{A,max}$. This particular design enables the relative motion between the sample surfaces in accordance to the rotary swaging process.

The test rig was applied for a first evaluation of the frictional properties of various tool samples (material 1.2379, hardness 62 HRC) under process specific conditions. The tool samples were a polished

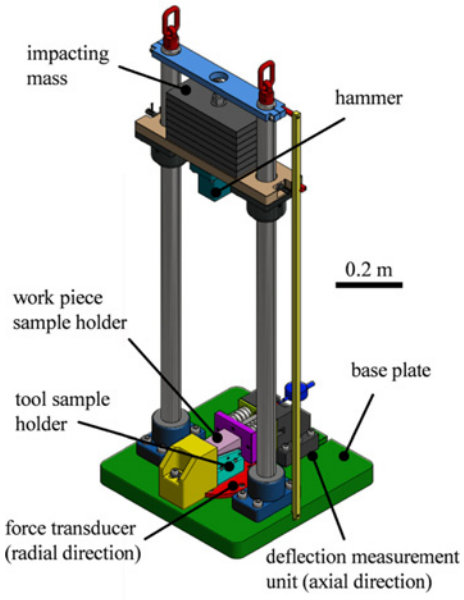


Fig. 5 Test rig for the tribological investigation of micro structured surfaces, reflecting the kimematic and loads of the rotary swaging process

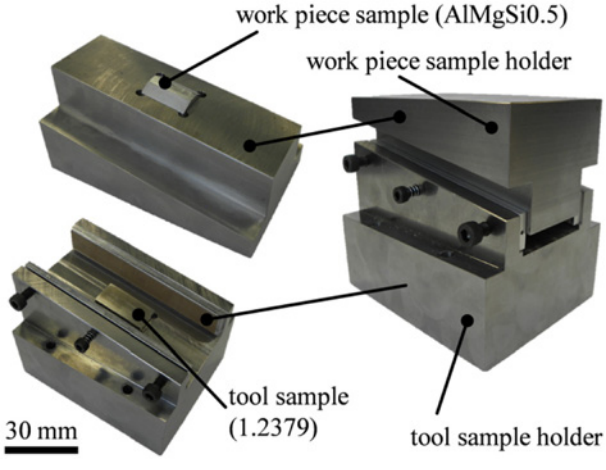


Fig. 6 Assembly of sample holders and samples for the test rig

reference sample, roughness Sa = 10 nm (tested lubricated and dry), a macro structured sample exhibiting a sinusoidal structure (amplitude 0.15 mm, wavelength 1.3 mm), and a Cr/CrN/WCx+CrCx/a-C:H:W/a-C:H hard coated sample (roughness Sa = 10 nm). The work piece samples were made from AlMgSi0.5 aluminum alloy. The targeted excitation force for all experiments was 230 kN corresponding to a pressure per unit area of 2300 N/mm$^2$ applied to the samples surfaces. Fig. 7 shows the measured maximum excitation force $F_{R,max}$ and maximum reaction force $F_{A,max}$ for each experimental variant. The measured maximum excitation force is less than the targeted excitation force due to deformation energy applied to the work piece samples. The deviation given is the minimum and maximum measured force of four single experiments per sample-surface combination. An assignment of the results to common friction models such as Coulomb's friction law or the friction factor model has not been carried out due to the particularities of the evaluation technique. These comprise dynamic loads, relative motion between the samples at the moment of excitation as well as plasticity of the work piece sample.

A high maximum reaction force of 50 kN in average was measured for the lubricated experiment with the polished reference tool sample. All dry experiments lead to considerably lower maximum reactions forces of below 10 kN what is linked to higher friction. The macro structured samples allowed to increase the friction compared to the polished sample under dry conditions and exhibits the lowest deviation in reaction forces measured. Contrary to expectations, greatest friction was identified for the hard coated tool sample. This first series of tests will be followed by comprehensive tribological investigation of various structured and hard coated surfaces to allow a correlation between the particular surface structure and the frictional properties in accordance to the specific conditions of rotary swaging.

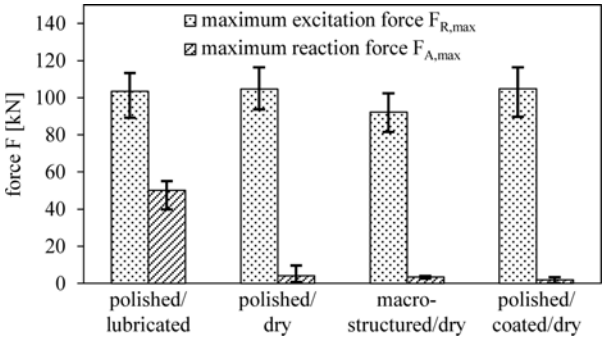


Fig. 7 Measured maximum excitation force $F_{R,max}$ and max-imum reaction force $F_{A,max}$ for various tool sample surfacesand conditions (lubricated/dry)

### 3.3 Process Modeling and Simulation

A further understanding of the rotary swaging process, e.g. the formation of process forces dependent on the tribological properties, is one major aspect for the pre-determination of adequate frictional surface properties of the tools as well as suitable process parameter such as process forces and feeding speed in order to provide robust dry forming processes. Even though investigations on the process forces and the energy requirement have been carried out, a complete understanding of the effect of the particular tribological conditions of the rotary swaging process so far has not been derived.[1] A finite element modeling (FEM) and simulation of the rotary swaging process is of great importance to overcome this limitations and helps to determine process forces, material flow and strain and stress distribution in the work piece.[17,18] Several investigations in literature have shown the impact of axial feed velocity, frictional properties and tool geometry on the rotary swaging process and the work piece. These studies lead to the formulation of the neutral plane (NP), where no axial flow of the material can be detected.[19] The material left or right of the NP flows in the backward or forward direction. Thus, the location of the NP represents the productivity, due to the fact that more or less material flows into the reduction zone dependent on the friction between the tools and the work piece. Therefore, FE modeling with respect to the NP concept is seen to be one key aspect in the development of the rotary swaging towards a lubricant free process design and is one discipline in the presented approach. Commonly two-dimensional axisymmetric simulations are performed for radial forging and rotary swaging.[17-19] The model for the rotary swaging is implemented with the software Simulia ABAQUS 6.13-1 and consists of two parts, tool and work piece (see Fig. 8).

The tool as a rigid body is split in two segments the reduction

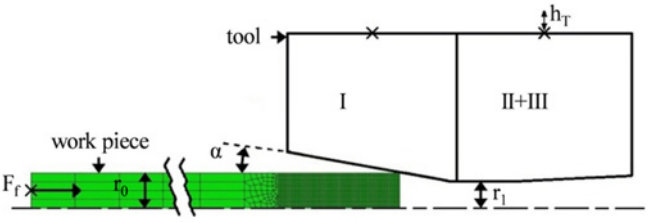


Fig. 8 2D-Axisymmetric-Model

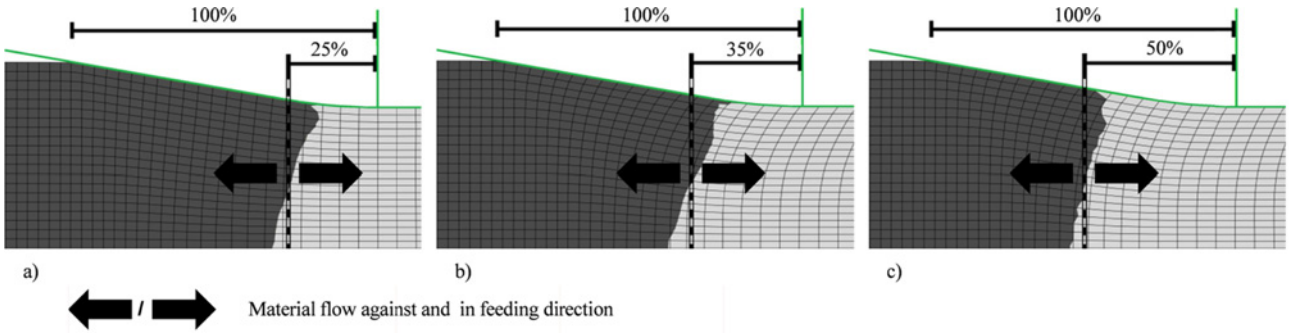


Fig. 9 Influence of the friction coefficient on the neutral plne; (a) $\mu_{Red}$ = 0.1, $\mu_{Cal}$ = 0.1 (b) $\mu_{Red}$ = 0.5, $\mu_{Cal}$ = 0.5 (c) $\mu_{Red}$ = 0.5, $\mu_{Cal}$ = 0.1. The dark gray area characterizes material flow to the left und the light gray area characterizes material flow to the right side

zone (I) and the calibration zone (II). The exit zone (III) is included in the second segment, as this zone has almost no contact to the work piece. Thus, the radial forces were analyzed separately. The numerical method is based on Abaqus/Explicit. The frictional behavior within the simulation was calculated based on Coulomb's law and the penalty formulation. The first simulations analyzed the effect of the friction coefficient value on the location of the neutral plane as shown in Fig. 9. For a low friction coefficient value in the reduction zone $\mu_{Red} = 0.1$ and the calibration zone $\mu_{Cal} = 0.1$ the distance of the neutral plane with respect to the calibration zone is 25% (see Fig. 9(a)). The complete contact length of tool and work piece in the forging zone is labeled as 100%. For a high friction coefficient value of $\mu_{Red/Cal} = 0.5$ the distance increases to a value of 35% (see Fig. 9(b)). Higher friction coefficient values lead to a better grip and therefore more material is formed into the feeding direction. The largest distance of the neutral plane to the calibration zone with a value of 50% was achieved with differing friction coefficient values for the tool zones (see Fig. 9(c)). The low friction coefficient value in the calibration zone facilitates the forming and the material flow at the surface in the calibration zone.

## 4. Conclusions

In this work three approaches are shown concertedly contributing to the development of a lubricant free rotary swaging process. These approaches deal with the adaption of the tools surfaces with regard to the tribological conditions between the tools and the work piece as well as with the process design regarding e.g. ideal process parameters using modeling and simulation techniques. Hard coatings show a clear potential to overcome issues of abrasive and adhesive tool wear in dry metal forming processes. Particularly tungsten doped a-C:H coatings provide high hardness for improved abrasion resistance and high toughness to withstand impact loads without crack formation and coating failure. These hard coatings are suitable for the application to rotary swaging tools. Furthermore, structured tool surfaces can contribute to a lubricant free rotary swaging by changing frictional conditions, especially in the reduction zone of the tools. The increase of friction through a work piece material interlocking with the structured tool surfaces is associated with a shift of the neutral plane and allows for an effective rotary swaging by reducing the axial reaction force. For the evaluation of the tribological effectiveness of such structures and hard coated surfaces a test rig was developed, replicating the contact geometries of the tool and work piece as well as impact loads. This test rig allows for comprehensive tribological testing regardless of the actual rotary swaging process. First experiments with the new test rig were conducted successfully and the tribological effectiveness of especially macroscopic structures was shown. At last, the successful implementation of a two-dimensional FE model of rotary swaging taking into account the macro and micro geometry, the frictional properties, and process kinematics was shown. Such a FE model can effectively be used for process layout and the simulative testing of the impact of structured or coated surfaces with varying frictional properties based on the formation and the determination of the neutral plane position as well as the calculation of the resulting process forces. All methods considered are steps straight forward into the development and implementation of lubricant free rotary swaging processes.

## ACKNOWLEDGEMENT

The authors would like to thank the German Research Foundation (DFG Deutsche Forschungsgemeinschaft) for funding this work within the sub-project "Potentials of Dry Rotary Swaging" of the priority program SPP 1676 "Dry metal forming - sustainable production through dry processing in metal forming."

## REFERENCES

1. Herrmann, M., Hasselbruch, H., Böhmermann, F., Kuhfuss, B., Zoch, H., et al., "Dry Metal Forming Open Access Journal," FMT 1, pp. 63-71, 2015.
2. Hetzner, H., "Systematische Entwicklung Amorpher Kohlenstoffschichten unter Berücksichtigung der Anforderungen der Blechmassivumformung," Ph.D. Thesis, Department of Engineering, University of Erlangen, 2014.
3. Spur, G. and Stöferle, T., "Handbuch der Fertigungstechnik Band 2/1 Umformen," Carl Hanser Verlag, pp. 85-94, 1983.
4. Ghiotti, A. and Bruschi, S., "Tribological Behaviour of DLC Coatings for Sheet Metal Forming Tools," Wear, Vol. 271, No. 9, pp. 2454-2458, 2011.
5. Liu, Y., Erdemir, A., and Meletis, E., "An Investigation of the Relationship between Graphitization and Frictional Behavior of DLC Coatings," Surface and Coatings Technology, Vol. 86-87, pp. 564-568, 1996.
6. Murakawa, M., Jin, M., and Hayashi, M., "Study on Semidry/Dry Wire Drawing using DLC Coated Dies," Surface and Coatings Technology, Vol. 177-178, pp. 631-637, 2004.
7. Carlsson, P. and Olsson, M., "PVD Coatings for Sheet Metal Forming Processes: A Tribological Evaluation," Surface and Coatings Technology, Vol. 200, No. 14, pp. 4654-4663, 2006.
8. Fujimoto, K., Yang, M., Hotta, M., Koyama, H., Nakano, S., et al., "Fabrication of Dies in Micro-Scale for Micro-Sheet Metal Forming," Journal of Materials Processing Technology, Vol. 177, No. 1, pp. 639-643, 2006.
9. Weber, M., Bewilogua, K., Thomsen, H., and Wittorf, R., "Influence of Different Interlayers and Bias Voltage on the Properties of aC: H and aC: H: Me Coatings Prepared by Reactive dc Magnetron Sputtering," Surface and Coatings Technology, Vol. 201, No. 3, pp. 1576-1582, 2006.
10. Chen, X., Peng, Z., Fu, Z., Wu, S., Yue, W., et al., "Microstructural, Mechanical and Tribological Properties of Tungsten-Gradually Doped Diamond-Like Carbon Films with Functionally Graded Interlayers," Surface and Coatings Technology, Vol. 205, No. 12, pp. 3631-3638, 2011.

11. Czyzniewski, A., "Optimising Deposition Parameters of W-DLC Coatings for Tool Materials of High Speed Steel and Cemented Carbide," Vacuum, Vol. 86, No. 12, pp. 2140-2147, 2012.

12. Fritz, B., "Forming Tool, in Particular Kneading Tool," International Patent No. WO 2010/105826 A1, 2010.

13. Franzen, V., Witulski, J., Brosius, A., Trompeter, M., and Tekkaya, A., "Textured Surfaces for Deep Drawing Tools by Rolling," International Journal of Machine Tools and Manufacture, Vol. 50, No. 11, pp. 969-976, 2010.

14. Arentoft, M., Bay, N., Tang, P. T., and Jensen, J., "A New Lubricant Carrier for Metal Forming," CIRP Annals-Manufacturing Technology, Vol. 58, No. 1, pp. 243-246, 2009.

15. Brinksmeier, E., Riemer, O., and Twardy, S., "Tribological Behavior of Micro Structured Surfaces for Micro Forming Tools," International Journal of Machine Tools and Manufacture, Vol. 50, No. 4, pp. 425-430, 2010.

16. Suh, N. P. and Saka, N., "Surface Engineering," CIRP Annals-Manufacturing Technology, Vol. 36, No. 1, pp. 403-407, 1987.

17. Pantalé, O. and Gueye, B., "Influence of the Constitutive Flow Law in Fem Simulation of the Radial Forging Process," Journal of Engineering, Vol. 2013, Article ID: 231847, 2013.

18. Li, R., Nie, Z.-R., and Zuo, T.-Y., "FEA Modeling of Effect of Axial Feeding Velocity on Strain Field of Rotary Swaging Process of Pure Magnesium," Transactions of Nonferrous Metals Society of China, Vol. 16, No. 5, pp. 1015-1020, 2006.

19. Moumi, E., Ishkina, S., Kuhfuss, B., Hochrainer, T., Struss, A., et al., "2D-Simulation of Material Flow during Infeed Rotary Swaging Using Finite Element Method," Procedia Engineering, Vol. 81, pp. 2342-2347, 2014.